The Global Fire Monitoring Center (GFMC)

Working Paper 1 / 2002

BIRD Detection of Coal Seam Fires in East Kalimantan, Indonesia

Boris Zhukov[1], Dieter Oertel[1] and Johann Georg Goldammer[2]
[1] DLR, Institut für Weltraumsensorik und Planetenerkundung, Rutherfordstr. 2
D-12489 Berlin, Germany
[2] Global Fire Monitoring Center (GFMC), Max Planck Institute for Chemistry and Freiburg University, Georges-Koehler-Allee 75, D-79110 Freiburg, Germany

This Working Paper contains first results of the Bi-spectral InfraRed Detection (BIRD) satellite detection and characterization of coal seam fires in East Kalimantan, Indonesia, in the area between Samarinda and Balikpapan. This area is known for its coal seam fires (Goldammer and Hoffmann 2001). The history and ecological significance of the co-ordinates of coal seam fires along the Samarinda-Balikpapan road and in Bukit Soeharto National Park have been investigated by Goldammer and Seibert (1989, 1990) and Goldammer et al. (1996) (see also Fig. 1). The co-ordinates of the currently burning coal seams have been made available by Mr. Alfred E. Whitehouse, Project Director of the Office of Surface Mining, Ministry of Energy and Mineral Resources, Mining Program Management Project (Jakarta, Indonesia). The hot areas are visible from the air or from space (Fig. 1) are relatively small, making their detection with BIRD rather problematic, unless the coal seam fires have a very high temperature (temperatures of up to a few thousand Kelvin were reported) or heat the surrounding surface or ignite the surrounding vegetation.

For this study, we used a fragment of the multispectral image obtained on 16 May 2002 by the DLR small satellite BIRD (Annex A). The fragment has a size of 500×800 sampling steps (185 m) and covers the Samarinda-Balikpapan area. Figures 2-4 show the band images in the Near-Infrared (NIR, 0.84-0.90 μm), Mid-Infrared (MIR, 3.4-4.2 μm) and Thermal-Infrared (TIR, 8.5-9.3 μm) spectral bands. The imaging was repeated on the next day, however then the area was nearly completely covered with clouds.

The scene is partly covered with many small clouds that are seen as bright in the NIR (Fig. 2) and dark in the TIR (Fig. 4). In the MIR (Fig. 3), the lower-level clouds are brighter while the cold higher-level clouds are darker the background.

The NIR image shows no sun glints in the region that could produce false alarms during the detection of High-Temperature Events (HTE).

In spite of the cloudiness, the MIR image allows to identify a number of bright surface features including:

- small HTE that are very bright in the MIR and in most cases not seen in the TIR, what indicates their relatively high temperature,

- larger areas that are brighter than the background both in the MIR and TIR, which correspond to warm surfaces.

The HTE may be vegetation fires or near-surface coal seam fires but also may have another, for instance, industrial origin. Three small HTE, which are observed in the sea, could be e.g. oil platforms.

Warm surfaces may be bare soils and fire scars heated by the sun (cooling fires with the temperature of above ~350 K are usually detected as HTE). Underground coal seam fires can also be considered as a possible heating source.

Figure 5 shows the location of the HTE that were recognised by the BIRD HTE detection algorithm (Annex B). They are colour-coded using their estimated energy release. For comparison, the locations of the documented coal seam fires are also shown with crosses. The resolution of the digital map that was used for geo-referencing of the BIRD image is ~0.02° in latitude and longitude (~1.8 km), resulting in a possible mis-location of the documented coal seam fires in the BIRD image of up to ~10 pixels. Only in one area, which is indicated in Fig. 4 with a circle; the distance of two detected HTE from the documented coal seam fires is within the geo-referencing accuracy of the BIRD image.

Warm surface are rejected by the BIRD HTE detection algorithm that recognises only hot targets.

A few reasons are possible for the non-compliance of the BIRD HTE detection and of the ground coal-seam fire mapping:
- Small size of typical coal fire outlets that does not allow their detection by BIRD
- Cloud coverage of many of the coal fire locations
- Time difference between the BIRD imaging and on-ground mapping of the coal seam fires

Table 1 gives the co-ordinates of the HTE detected in the BIRD data (with the geo-referencing accuracy of ~0.02 deg), as well as their equivalent fire temperature and area and the energy release. In most of the cases, the fire temperature and area estimations for these small HTE are not stable relative the TIR background estimation error (see Annex B), resulting e.g. in the temperature error intervals that cover the entire temperature range of active and cooling fires (here it is conventionally limited from above by 1200 K). Only for a few larger HTE (No 4, 6, 9, 14, 17), relatively stable estimations of the equivalent fire temperature were obtained giving the values from 370 to 550 K. Similar values were obtained during BIRD coal seam fire observations in China. They indicate that warm surface contribution dominates over the contribution of high-temperature areas in the radiation of the detected HTE.

The energy release estimations are in many cases more stable than the estimations of the fire temperature and area. The energy release of the detected HTE ranges from 1 MW to over 10 MW according to the Bi-spectral method (the adapted MODIS method leads to a strong energy release under-estimation when the fire temperature is below ~500 K).

A further closer on-ground or airborne inspection is strongly recommended to validate the presented results of HTE recognition that was based on the BIRD data.

References

Goldammer, J. G., and B. Seibert. 1989. Natural rain forest fires in Eastern Borneo during the Pleistocene and Holocene. Naturwissenschaften 76, 518-520.

Goldammer, J. G., and B. Seibert. 1990. The impact of droughts and forest fires on tropical lowland rain forest of Eastern Borneo. In: Fire in the tropical biota. Ecosystem processes and global challenges (J.G. Goldammer, ed.), 11-31. Ecological Studies 84, Springer-Verlag, Berlin-Heidelberg-New York, 497 p.

Goldammer, J. G., B. Seibert, and W. Schindele. 1996. Fire in dipterocarp forests. In: Dipterocarp forest ecosystems: Towards sustainable management (A. Schulte and D. Schöne, eds.), 155-185. World Scientific Publ., Singapore-New Jersey-London-Hong Kong, 666 pp.

Goldammer, J. G., and A. A. Hoffman, 2001. Fire situation in Indonesia. In: FRA Global Forest Fire Assessment 1990-2000. Forest Resources Assessment Programme, Working Paper 55, p. 132-144. FAO, Rome, 495 p.

Oertel, D., K. Briess, W. Halle, M. Neidhardt, E. Lorenz, R. Sandau, F. Schrandt, W. Skrbek, H. Venus, I. Walter, B. Zender, B. Zhukov, J.G. Goldammer, A.C. Held, M. Hille, and H. Brueggemann. 2002. Airborne forest fire mapping with an adaptive infrared sensor. Int. J. Remote Sensing 24, 3663-3682.

Tab. 1. Characteristics of the HTE detected in the BIRD image of East Kalimantan

N	Centre co-ordinates		Equivalent fire temperature, K	Equivalent fire area, Ha	Fire proportion, %	Energy release, MW	
	Latitude, N., deg.	Longitude, E., deg.				Bi-spectral method	Adapted MODIS method
1	-0.17	117.36	818 (363-1200)	0.004 (0.001-1.441)	0.011 (0.002-4.679)	0.9 (0.8-7.7)	1.1
2	-0.22	116.95	- (446-1200)	- (0.001-0.183)	- (0.002-0.595)	2.0 (0.8-3.2)	1.1
3	-0.33	116.99	460 (382-1200)	0.213 (0.001-1.203)	0.414 (0.002-2.344)	4.3 (1.3-8.8)	1.6
4	-0.36	117.43	428 (376-622)	0.459 (0.028-1.701)	0.894 (0.054-3.313)	6.4 (2.7-10.8)	1.8
5	-0.34	116.99	499 (408-1200)	0.199 (0.002-1.117)	0.264 (0.003-1.484)	6.0 (2.3-12.2)	2.9
6	-0.35	117.07	416 (369-569)	0.402 (0.033-1.435)	1.307 (0.108-4.660)	4.8 (2.1-8.0)	1.2
7	-0.42	117.09	478 (381-1200)	0.104 (0.001-0.842)	0.336 (0.002-2.733)	2.6 (0.9-6.0)	1.1
8	-0.47	117.43	686 (477-1200)	0.009 (0.001-0.109)	0.023 (0.002-0.266)	1.1 (0.9-2.7)	1.1
9	-0.45	116.96	373 (337-557)	2.104 (0.065-8.703)	5.123 (0.158-21.192)	12.9 (4.6-23.0)	2.0
10	-0.46	117.13	386 (337-1200)	1.801 (0.002-10.459)	2.288 (0.002-13.286)	14.2 (2.2-29.6)	2.5
11	-0.45	116.95	393 (344-1200)	0.792 (0.001-4.100)	2.570 (0.003-13.310)	6.9 (1.2-13.3)	1.4
12	-0.51	117.62	- (956-1200)	- (0.001-0.003)	- (0.002-0.005)	1.6 (1.5-1.6)	2.0
13	-0.51	117.61	661 (567-1023)	0.013 (0.002-0.033)	0.041 (0.005-0.108)	1.3 (1.0-1.8)	1.2
14	-0.57	117.08	378 (349-442)	1.912 (0.420-5.271)	3.492 (0.768-9.625)	12.9 (7.0-18.9)	2.2
15	-0.59	117.20	414 (344-1200)	0.684 (0.001-5.582)	1.333 (0.003-10.874)	8.1 (1.7-18.9)	2.0
16	-0.59	117.08	- (416-1200)	- (0.001-0.670)	- (0.002-1.088)	4.9 (1.6-8.2)	2.0
17	-1.01	117.53	551 (479-822)	0.055 (0.005-0.156)	0.107 (0.011-0.304)	2.6 (1.5-3.9)	1.7
18	-0.99	117.16	493 (355-1200)	0.296 (0.003-7.071)	0.377 (0.004-8.983)	8.5 (3.2-32.1)	3.7
19	-1.21	116.78	- (331-1200)	- (0.001-7.746)	- (0.002-14.145)	10.7 (1.2-20.1)	1.5
20	-1.22	116.95	- (395-1200)	- (0.001-0.865)	- (0.002-1.685)	4.6 (1.3-7.9)	1.6

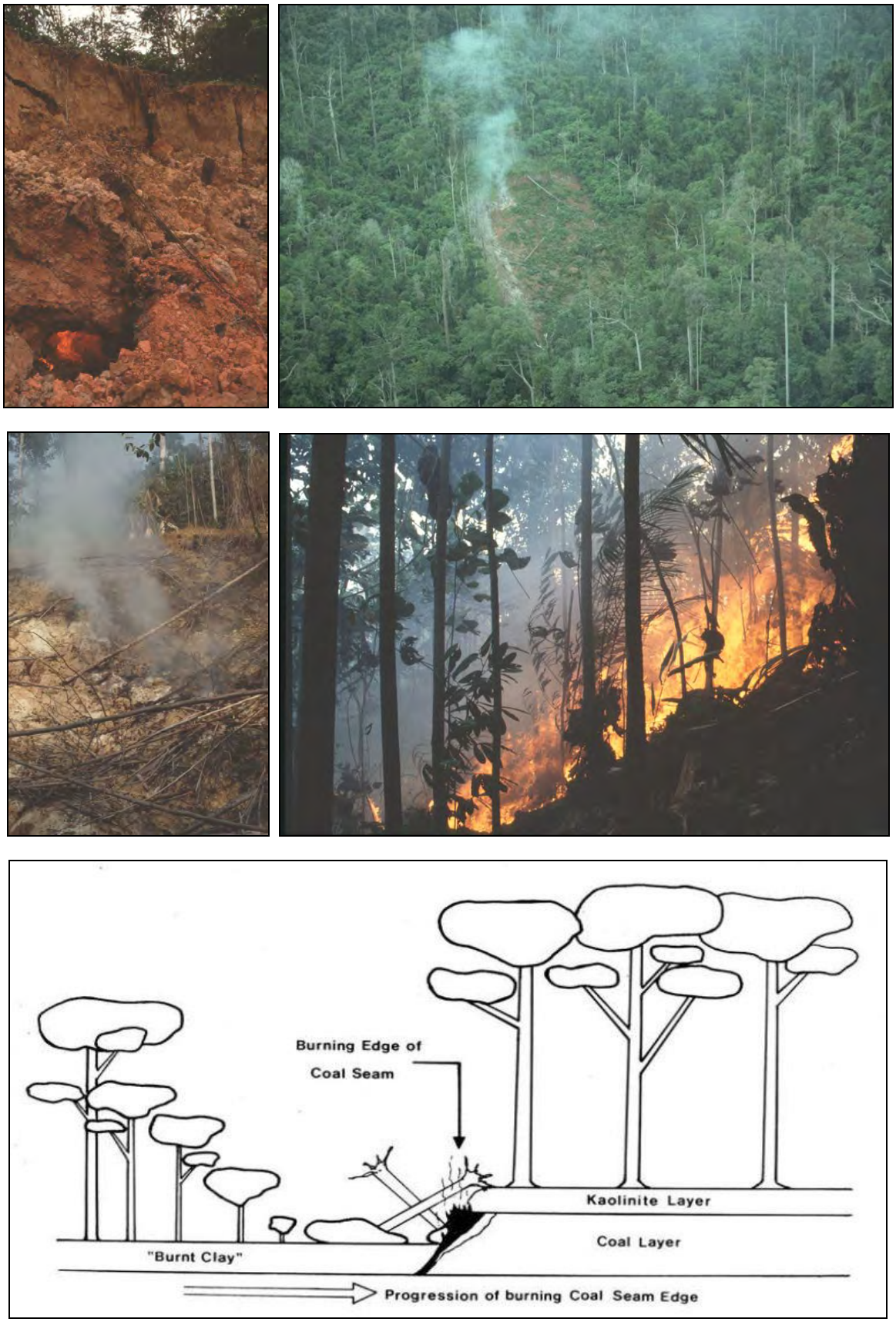

Fig. 1. Ground and aerial photographs of coal seam fires in Bukit Soeharto National Park, East Kalimantan (between the Samarinda and Balikpapan). The lower graph shows the slow progression of a burning coal seam through the primary rain forest with the consequence of starting a forest fire during a drought period such as caused by a strong El Niño (Photos: GFMC; graph from Goldammer and Seibert, 1989)

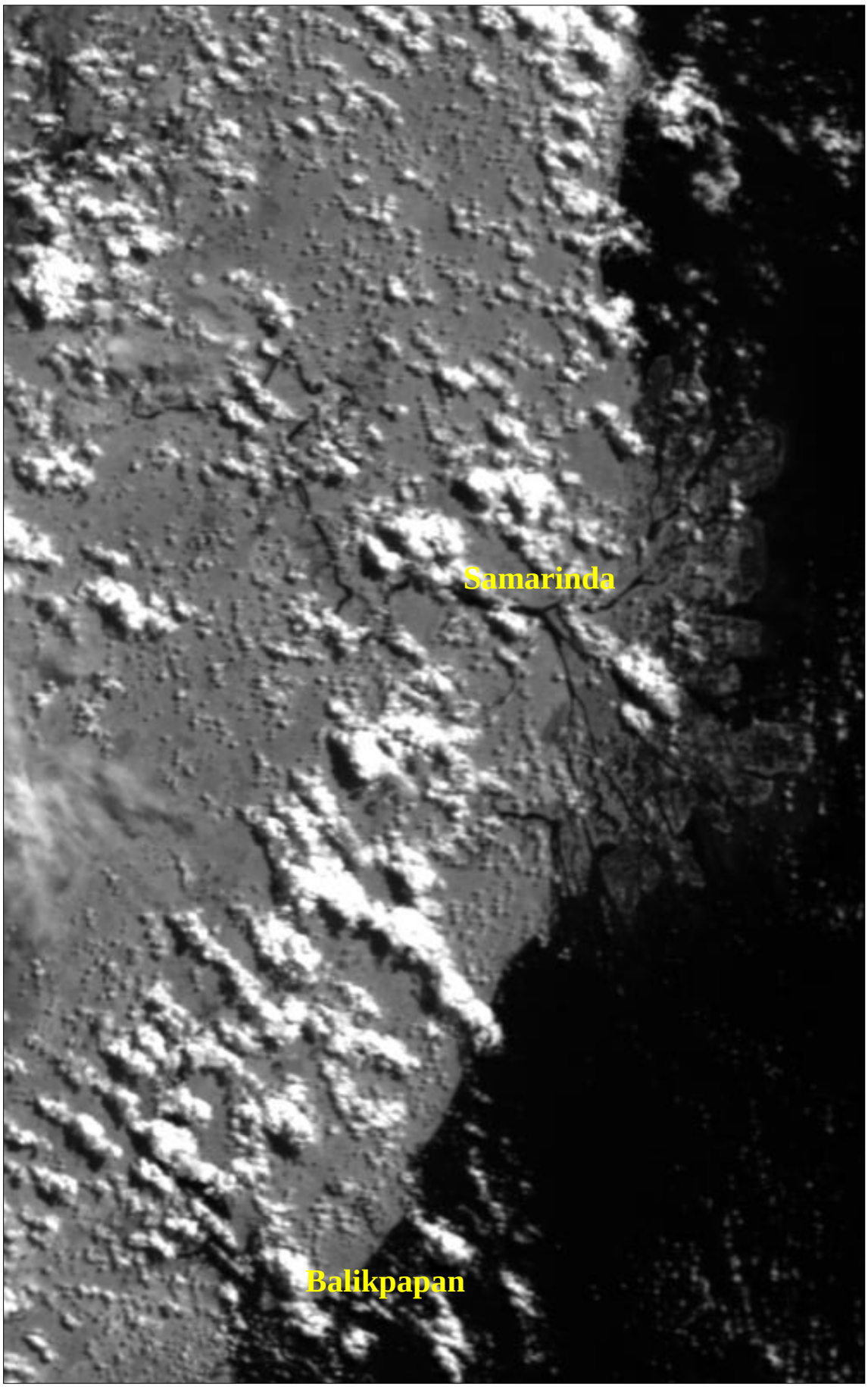

Fig. 2. BIRD image of the East Kalimantan, Indonesia: NIR channel

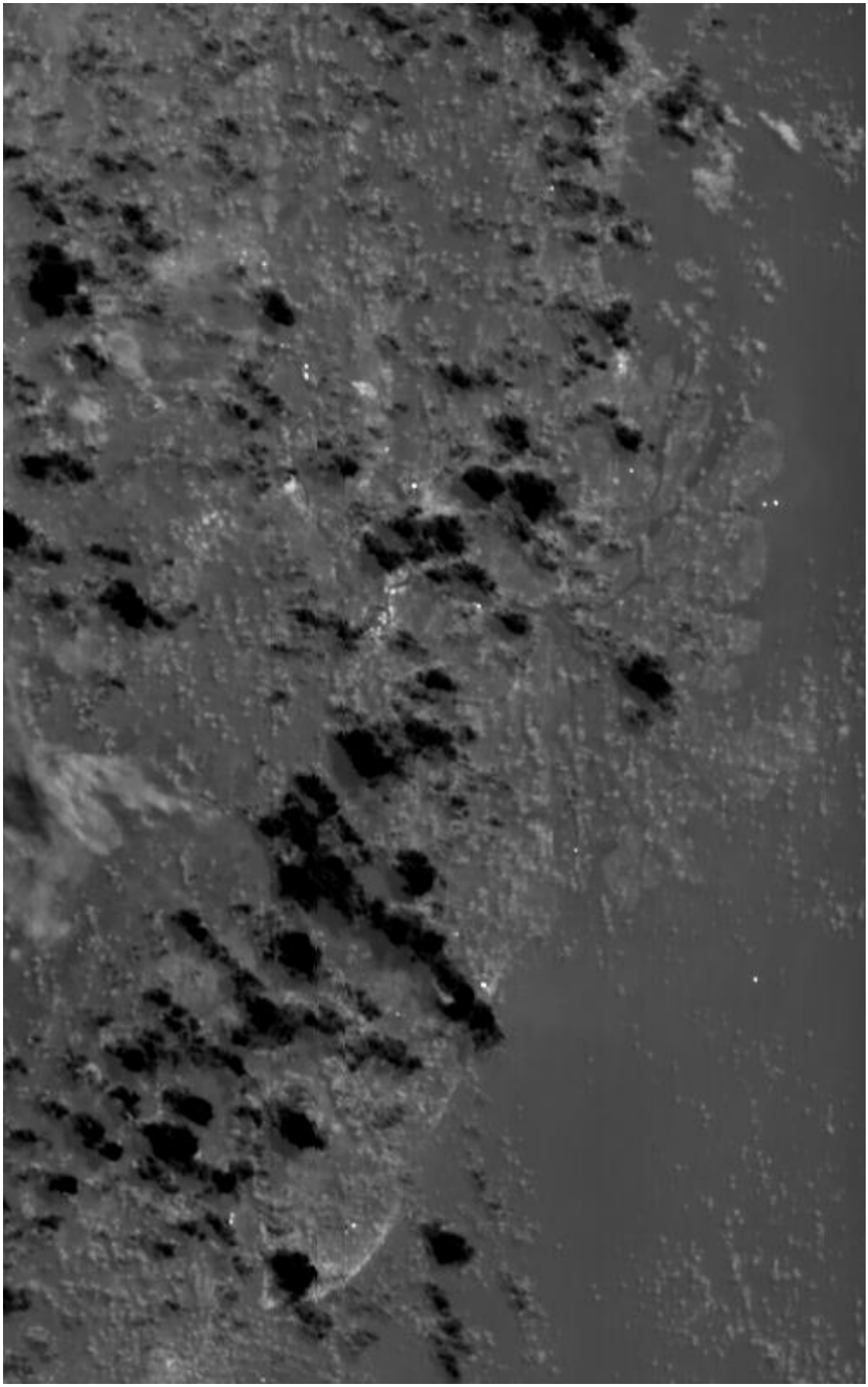

Fig. 3. BIRD image of the East Kalimantan, Indonesia: MIR channel

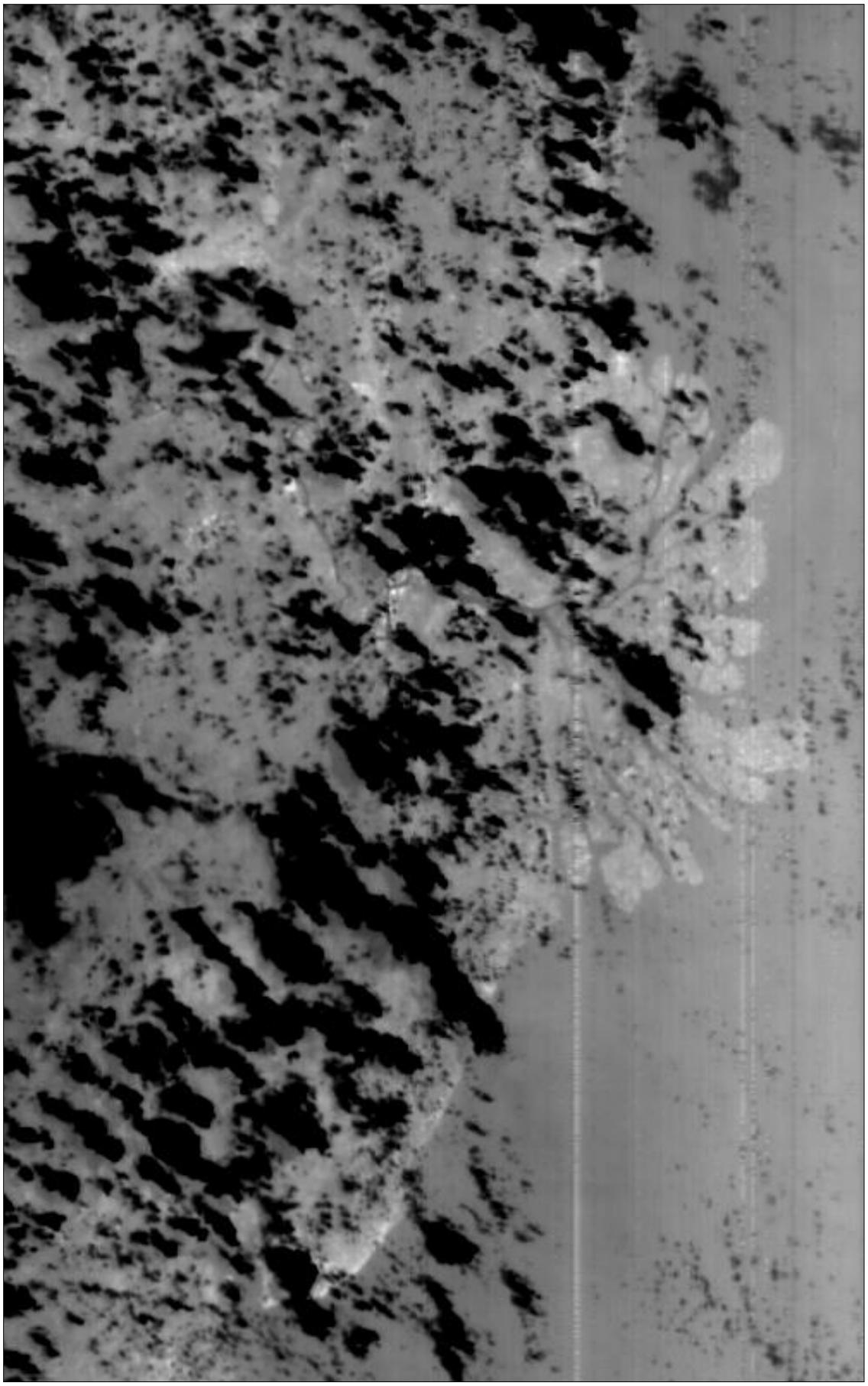

Fig. 4. BIRD image of the East Kalimantan, Indonesia: TIR channel

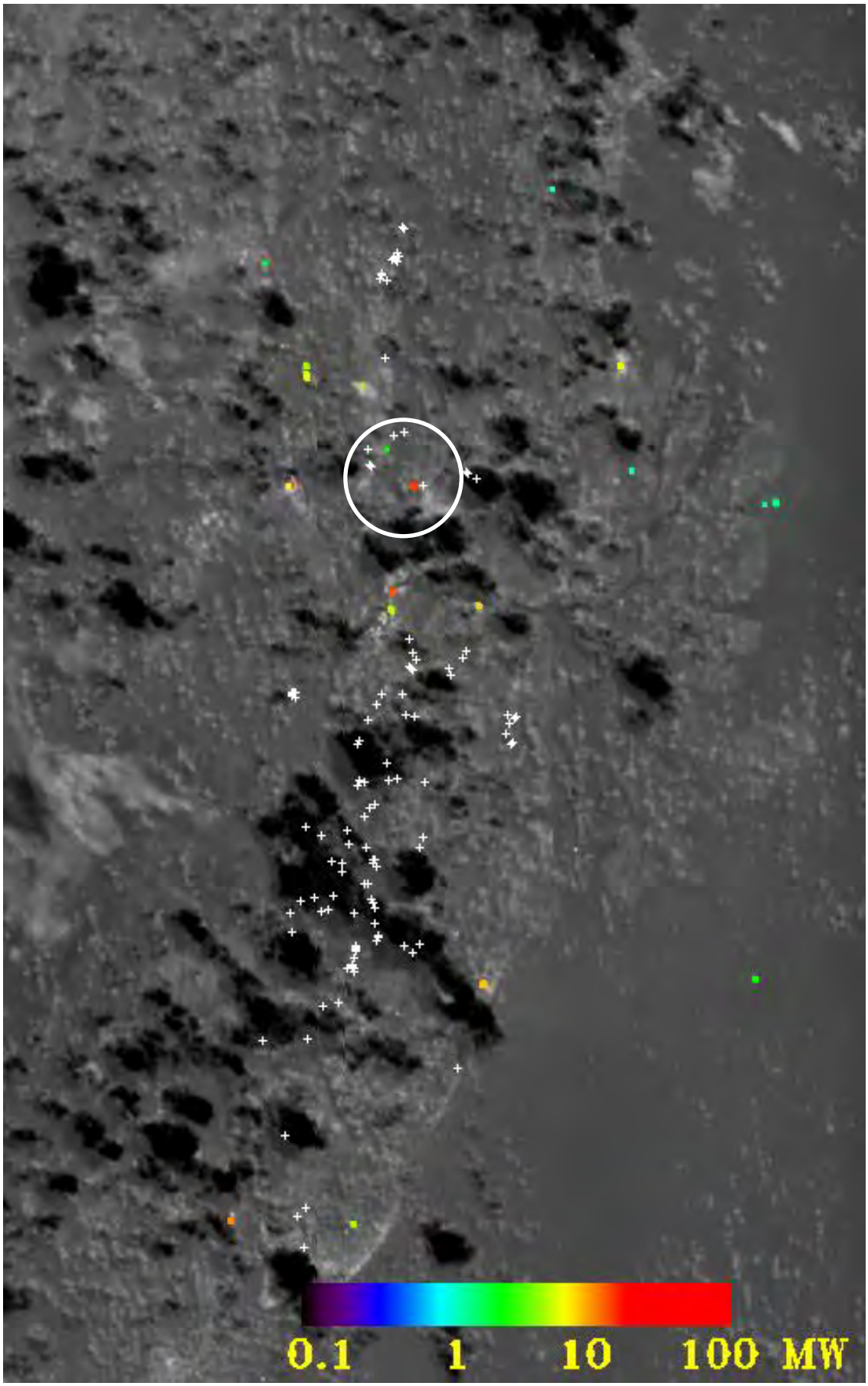

Fig. 5. Detected HTE in the BIRD image and their energy release (crosses show the location of the documented coal seam fires)

ANNEX A

Short description of the Bi-spectral Infrared Detection Mission and the BIRD main sensors

The BIRD small satellite mission is a technology demonstrator of new infrared push-broom sensors dedicated to recognition and quantitative characterization of thermal processes on the Earth surface. BIRD primary mission objectives are (Briess et al., 1996):

- Test of a new generation of infrared array sensors with an adaptive radiometric dynamic range,
- Detection and scientific investigation of High Temperature Events (HTE) such as forest fires, volcanic activities, and coal seam fires,
- Test of small satellite technologies, such as an attitude control system using new star sensors and new actuators, an on-board navigation system based on a new orbit predictor and others.

The BIRD main sensor payload consists of:

- A two-channel infrared Hot Spot Recognition Sensor system (HSRS)
- A Wide-Angle Optoelectronic Stereo Scanner (WAOSS-B)

Their characteristics are given in Table 1.

Tab. 1. Characteristics of the BIRD main sensor payload

	WAOSS-B	**HSRS**
Spectral bands	VIS: 600-670nm NIR: 840-900nm	MIR: 3.4-4.2µm TIR: 8.5-9.3µm
Focal length	21.65mm	46.39mm
Field of view	50°	19°
f-number	2.8	2.0
Detector	CCD lines	CdHgTe Arrays
Detector cooling	Passive, 20°C	Active, 80-100 K
Pixel size	7µmx7µm	30µmx30µm
Pixel number	2880	2x512 staggered
Quantization	11bit	14bit* exposure)
Ground pixel size	185m	370m
Sampling step	185m	185m
Swath width	533km	190km

* for each exposure

HSRS is a two-channel push-broom scanner with spectral bands in the mid-infrared (MIR) and thermal infrared (TIR) spectral ranges (Skrbek and Lorenz, 1998). The sensitive devices are two Cadmium Mercury Telluride (CdHgTe) photodiode lines. The lines – with identical layout in the MIR and TIR – comprise 2 x 512 elements each in a staggered structure. HSRS sensor head components of both spectral channels are based on identical technologies to

provide good pixel co-alignment. Both spectral channels have the same optical layout but with different wavelength-adapted lens coatings.

The detector arrays are cooled to 100 K in the MIR and to 80 K in the TIR. The cooling is conducted by small Stirling cooling engines. The maximal TIR photodiode cut-off wavelength of about 10.5 μm, which can be achieved at 80 K, on one hand and the atmospheric ozone band at 9.6 μm on the other hand require to use the 8.5 – 9.3 μm band for TIR channel of the HSRS instead of the usual 10.5 – 11.7 μm band. The HSRS sensor data are read out continuously with a sampling interval that is exactly one half of the pixel dwell time. This time-controlled "double sampling" and the staggered line array structure provide the sampling step that is a factor of 2 smaller than the HRSR pixel size, coinciding with the sampling step of the WAOSS NIR nadir channel.

Radiometric investigations of thermal anomalies require (a) a large dynamic range not to be saturated by HTE occupying the entire pixel and (b) a high signal to noise ratio to be able to observe small thermal anomalies at normal temperatures and detect small sub-pixel HTE. To fulfil these requirements, a second scene exposure is performed with a reduced integration time (within the same sampling interval!) if the real-time processing of the first exposure indicates that detector elements are saturated or close to saturation. As a result, the efficient HSRS radiometric dynamic range is significantly expanded keeping a very good temperature resolution at normal temperatures.

WAOSS-B is a modified version of a scanner that was originally developed for the Mars-96 mission. It is a three-line stereo scanner working in the push-broom mode. All three detector lines are located in the focal plane of a single wide angle lens. The forward- and backward-looking lines have a visible (VIS) and near-infrared (NIR) filters, respectively, while the nadir-looking line has a NIR filter.

Due to a higher resolution of the BIRD MIR and TIR channels in comparison to AVHRR and MODIS, it allows to achieve an order of magnitude smaller minimal detectable fire area. A possibility to observe fires and other HTE without sensor saturation provides: (a) an improved false alarm rejection capability and (b) a possibility of a quantitative estimation of HTE parameters (temperature, area, energy release) unrestricted by sensor saturation.

References to Annex A

Briess, K., H. Jahn, H.P. Roeser. 1996. A DLR Small Satellite Mission for the Investigation of Hot Spots, Vegetation and Clouds. *Acta Astronautica*, 39, 899-908.

Skrbek, W., and E. Lorenz. 1998. HSRS – An Infrared Sensor for Hot Spot Detection. *Proceedings of SPIE, Infrared Spaceborne Remote Sensing VI*, Vol. 3437, 167-176.

ANNEX B

HTE detection and quantitative characterisation

The BIRD high-temperature events (HTE) detection algorithm (Zhukov and Oertel, 2001) includes the following tests:

- Adaptive MIR thresholding to detect potential hot pixels,
- NIR thresholding to reject strong sun glints,
- Adaptive MIR/NIR radiance ratio thresholding to reject weaker sun glints, clouds and other high-reflective objects,
- Adaptive MIR/TIR radiance ratio thresholding to reject warm surfaces,
- Clustering of adjacent hot pixels, retrieval of the equivalent fire temperature and area and estimation of the fire energy release.

The equivalent fire temperature T_F and area A_F are the temperature and area of a homogeneous fire at a uniform background that would produce the same MIR and TIR radiances as the actual non-homogeneous fire. They are estimated using the Bi-spectral technique (Dozier, 1981). In contrast to the usual application of the Bi-spectral technique, we apply it not to separate hot pixels but to clusters of adjacent hot pixels (HTE). The advantages of the cluster-level retrievals are:

- the equivalent fire area A_F does not depend on the point spread function (PSF) of the MIR and TIR channels,
- the estimations of T_F and A_F are low-sensitive to small inter-channel MIR/TIR geometric co-registration errors and MIR/TIR PSF difference.

In order to account for sub-pixel co-registration errors of the MIR and TIR channels and PSF 'wings', the pixels located within a distance of 1 sampling step from the detected hot pixels are also included in the corresponding hot cluster.

T_F and A_F are found by solving the system of two equations:

$$\begin{aligned} &\bar{I}_{MIR} = \bar{q}_F B_{MIR}(T_F) + (1-\bar{q}_F) I_{MIR,bg}, \\ &\bar{I}_{TIR} = \bar{q}_F B_{TIR}(T_F) + (1-\bar{q}_F) I_{TIR,bg}, \end{aligned} \quad (1)$$

where $\bar{I}_{MIR}$ and $\bar{I}_{TIR}$ are the atmospherically-corrected mean MIR and TIR pixel radiances in a hot cluster, $B_{MIR}(T_F)$ and $B_{TIR}(T_F)$ are the band-integrated Planck function for the BIRD MIR and TIR channels, $\bar{q}_F$ is the mean fire proportion in the signal of cluster pixels that is related to the equivalent fire area as $\bar{q}_F = A_F / (A_{sampl} n_{pix})$, where n_{pix} is the number of pixels in a hot cluster, A_{sampl} = 3.42·10^4 m^2 is the BIRD sampling area that is defined as the square of the BIRD sampling step of 185 m. The BIRD sampling area is a factor of 4 smaller than the pixel area of its MIR and TIR channels due to the double sampling in the along-track and cross-track directions.

The MIR and TIR radiances of the background within a hot cluster $I_{MIR,bg}$ and $I_{TIR,bg}$ are estimated as the mean radiances $\bar{I}_{MIR,bg}$ and $\bar{I}_{TIR,bg}$ of background pixels in the vicinity of the hot cluster. However, since the TIR channel is relatively low sensitive to small sub-pixel fires, errors in the estimated TIR background radiance may lead to large errors in T_F and A_F. The effect of the MIR background errors is much smaller and can be neglected. In order to characterise the stability of the Bi-spectral retrievals to the TIR background radiance error, $I_{TIR,bg}$ was varied in the range of $\pm\sigma_{TIR,bg}$ around its nominal value of $\bar{I}_{TIR,bg}$, where $\sigma_{TIR,bg}$ is the standard deviation of the TIR background radiance in the vicinity of the hot cluster. As a result, error intervals for T_F and A_F are obtained along with their nominal values that correspond to $I_{TIR,bg} = \bar{I}_{TIR,bg}$. The width of these error intervals depends on the fire temperature, on the fire proportion in the cluster and on background variability.

When the TIR background radiance is overestimated, it may lead to unrealistically large values of T_F for small fires that have the TIR pixel radiance close to the background. In order to account for this effect, the upper limit of 1200 K was accepted for the equivalent fire temperature. If this limit is exceeded during the nominal estimation of T_F, the retrievals are considered as failed. If it is exceeded during the estimation of the upper bound for T_F, the upper bound is set to 1200 K and the corresponding lower bound for A_F is adjusted to this temperature. However, a possibility is also left to analyse objects with a temperature higher than 1200 K in the case when the Bi-spectral retrievals are relatively stable. For this purpose, the temperature limitation is not used if the mean TIR radiance of a hot cluster $\bar{I}_{TIR}$ exceeds $\bar{I}_{TIR,bg} + 3\sigma_{TIR,bg}$.

A more stable parameter for a quantitative characterisation of fires is their radiative energy release. It is useful for a parameterisation of the amount of burning vegetation, as well as for practical fire fighting purposes where the energy release per a unit length of a fire front characterises the front strength.

We compared two methods of radiative energy release estimation: the Bi-spectral technique and the MODIS method (Kaufman et al, 1998).

The Bi-spectral technique, which provides the equivalent fire temperature T_F and area A_F, allows an estimation of the energy release of a hot cluster relative to the background level as:

$$P_{BS} = \sigma(T_F^4 - T_{bg}^4)A_F \text{ ,(2)}$$

where σ is the Stefan-Boltzmann constant, T_{bg} is the background temperature that is assumed to be equal to the mean at-surface TIR temperature in the vicinity of the hot cluster. The error intervals for T_F and A_F define also the error interval for the fire energy release. The errors in T_F and A_F, which originate from the TIR background uncertainty, partly compensate each other. As a result, an acceptable error interval for the energy release can often be obtained if the error intervals for T_F and A_F are too large for a quantitative analysis.

The original MODIS method relates the radiative energy release of a fire pixel to its brightness temperature in the MODIS MIR channel at 3.9 μm. The method was adapted to energy release estimation of hot clusters in BIRD images as:

$$P_{MODIS} = k \cdot 4.34 \cdot 10^{-19} A_{sampl} \sum (T_{MIR}^8 - T_{MIR,bg}^8) \text{ [W]}, \quad (3)$$

where T_{MIR} and $T_{MIR,bg}$ are the BIRD MIR temperatures of a hot pixel and of the background in Kelvin, A_{sampl} is the BIRD sampling area and the sum is taken over all pixels in a hot cluster. The constant factor of $4.34 \cdot 10^{-19}$ was obtained in (Kaufman et al, 1998) from simulations of typical fire scenes. In order to be able to apply the MODIS method to the BIRD MIR band, a correction factor $k = 0.905$ was introduced in relation (3). It was defined from the regression of the cluster energy release as obtained by the Bi-spectral and MODIS methods (sec. Fig. 5 below).

An advantage of the Bi-spectral method of energy release estimation is that it accounts for the fire temperature. The advantage of the MODIS method is its better stability for small fires.

Additional offsets in the estimated hot cluster parameters are possible due to sensor calibration errors and errors in accounting for the atmospheric effects and for fire emissivity. Their effect on the Bi-spectral retrievals is usually significantly smaller than the effect of the TIR background error, except for large fires. For example, if each of these errors in the MIR and TIR channels is within 5-10%, then they cause a summed error in the equivalent fire temperature that increases from 15-30 K at T_F = 500 K to 60-120 K at T_F = 1000 K (Zhukov and Oertel, 2001).

References to Annex B

Kaufman, Y.J., C.O. Justice, L.P. Flynn. 1998. Potential global fire monitoring from EOS-MODIS. *Journal of Geophysical Research* **103**, 32215-32238.

Zhukov, B., and D. Oertel. 2001, Hot Spot Detection and Analysis Algorithm for the BIRD Mission, *Algorithm Theoretical Basic Document (ATBD), DLR-Berlin.*

ANNEX C

The following two viewgraphs show:

- A BIRD MIR image fragment with an overlay of the Fire Radiative Energy (FRE) release of the peat fires observed by BIRD in Indonesia Kalimantan (Souths of Borneo) in August 2002
- A comparison of BIRD and MODIS (Terra) images with the indication of the peat fires

Comments

1. The blue lines show the melioration channels – to dry out the region for consecutive land use change by application of fire – one of the reasons for the extended episode of peat and

forest fires with resulting severe regional air pollution during the El Niño in 1997-1998 (Heil and Goldammer, 2001)

2. The nearly simultaneous records of MODIS (Terra) and BIRD data of such relatively stable burning fires, like peat fires allow the „fine characterisation“ of the fire parameters via BIRD and a validation of MODIS data based fire radiative energy release (FRE).

Based on this „MODIS to BIRD FRE validation“, an extrapolation seems possible for the estimates of FRE obtained twice a day from MODIS (Terra) data when BIRD observation is not possible.

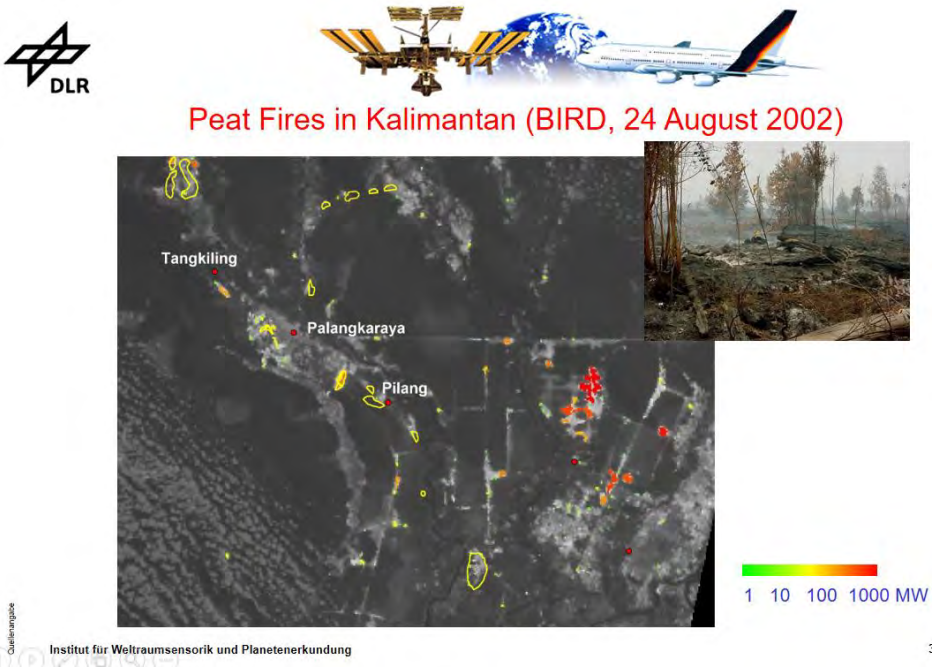

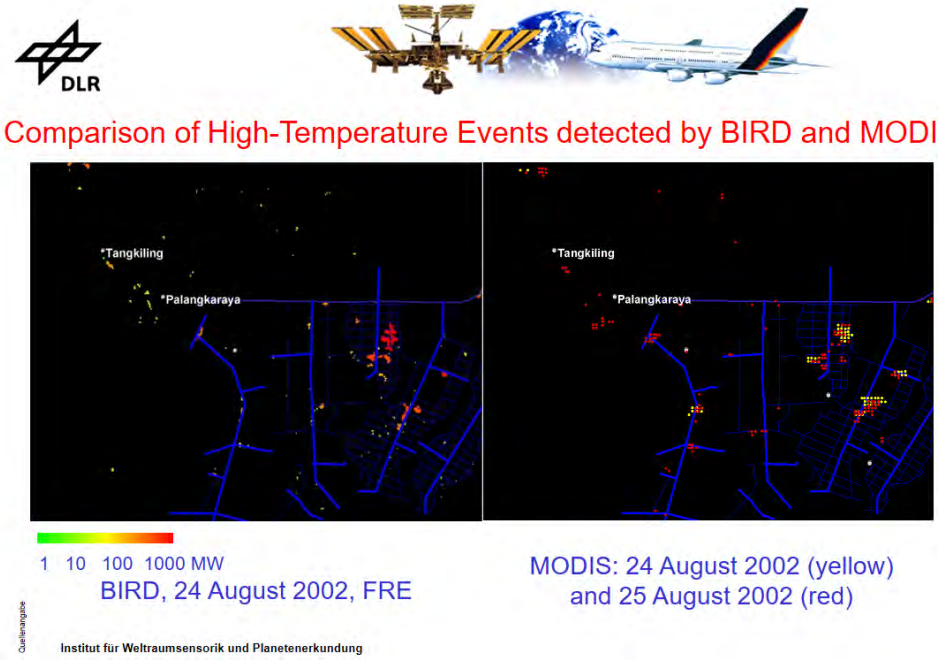

Reference to Annex C

Heil, A., and J.G. Goldammer. 2001. Smoke-haze pollution: a review of the 1997 episode in Southeast Asia. Regional Environmental Change 2 (1), 24-37.